Am J Physiol Heart Circ Physiol 291: H756–H761, 2006.
First published April 14, 2006; doi:10.1152/ajpheart.00063.2006.

Sodium current function in adult and aged canine atrial cells

Shigeo Baba,* Wen Dun,* Masanori Hirose, and Penelope A. Boyden

Department of Pharmacology, Center for Molecular Therapeutics, Columbia University, New York, New York

Submitted 17 January 2006; accepted in final form 17 March 2006

Baba, Shigeo, Wen Dun, Masanori Hirose, and Penelope A. Boyden. Sodium current function in adult and aged canine atrial cells. *Am J Physiol Heart Circ Physiol* 291: H756–H761, 2006. First published April 14, 2006; doi:10.1152/ajpheart.00063.2006.—The incidence of atrial fibrillation increases with age, but it is unknown whether there are changes in the intrinsic function of Na^+ currents in cells of the aged atria. Thus, we studied right (RA) and left (LA) atrial cells from two groups of dogs, adult and aged (>8 yr), to determine the change in Na^+ currents with age. In this study all dogs were in normal sinus rhythm. Whole cell voltage clamp techniques were used to compare the Na^+ currents in the two cell groups. Immunocytochemical studies were completed for the Na^+ channel protein $Na_v1.5$ to determine whether there was structural remodeling of this protein with age. In cells from aged animals, we found that Na^+ currents are similar to those we measured in adult atria. However, Na^+ current (I_{Na}) density of the aged atria differed depending on the atrial chamber with LA cell currents being larger than RA cell currents. Thus with age, the difference in I_{Na} density between atrial chambers remains. I_{Na} kinetic differences between aged and adult cells included a significant acceleration into the inactivated state and an enhanced use-dependent decrease in peak current in aged RA cells. Finally, there is no structural remodeling of the cardiac Na^+ channel protein $Na_v1.5$ in the aged atrial cell. In conclusion, with age there is no change in I_{Na} density, but there are subtle kinetic differences contributing to slight enhancement of use dependence. There is no structural remodeling of the fast Na^+ current protein with age.

ion channels; remodeling; arrhythmias; atrial fibrillation; age

ATRIAL FIBRILLATION occurs very often in the elderly patient. Recently, we have learned that aging alone is associated with significant heterogeneity of the atrial action potential (AP) duration (APD) and conduction parameters (1, 2, 8, 11). In adult and old dogs, aging is associated with a significant increase in P-wave duration, a reduction in maximum upstroke velocity (V_{max}), and total AP amplitude as well as a significant interregional variability of V_{max} (1). These data suggest that aging-associated changes in ionic currents underlying V_{max} of these multicellular AP studies may be spatially heterogeneous. Accordingly, because a major contributor of V_{max} is the fast Na^+ current (I_{Na}), we studied the Na^+ currents of right (RA) and left (LA) atrial cells of adult dogs and compared them to those of RA and LA cells from aged dogs (>8 yr) to see whether intrinsic changes in Na^+ currents could contribute to age-related changes in atrial electrophysiology.

METHODS

Cell preparation. This investigation conforms with the *Guide for the Care and Use of Laboratory Animals*, published by the National Institutes of Health (NIH Publication No. 85-23, Revised 1996). All protocols were reviewed and approved by the Institutional Animal Care and Use Committee. Dogs were anesthetized with pentobarbital sodium (30 mg/kg iv) and hearts removed via a thoracotomy. A section of one region, RA freewall, was excised for myocyte studies to minimize the known heterogeneity in regional ion channel function reported for normal canine atria (7). RA tissues were removed from adjacent sites for study of cellular electrophysiological properties. AP data have been reported previously (1, 2). From the same heart, a section of LA freewall was excised for studies of LA cell I_{Na} function.

Two groups of mongrel dogs (16–22 kg) were studied; adults (2–5 yr, adult dogs, $n = 23$) and old (>8 yr, aged dogs, $n = 21$). As in companion studies, ages were estimated during physical examination. These aged dogs, while all in normal sinus rhythm, had increased P-wave duration as reported previously (1, 2). Ages of dogs were estimated by a veterinarian based on standard measures of age, including dentition, eyes, coat, and musculoskeletal descriptors (1, 2).

Myocyte preparation. Single calcium-tolerant atrial cells were dispersed by using a modification of our previously described method (12). Briefly, the tissue was rinsed twice in a Ca^{2+}-free solution containing (in mM) 115 NaCl, 5 KCl, 35 sucrose, 10 dextrose, 10 HEPES, and 4 taurine (pH 6.95) and triturated in 20 ml of enzyme-containing solution (collagenase-II, 0.13 mg/ml at 36–37°C, Worthington Biochemical) for 30 min. Afterward, this solution was then decanted and discarded. The second trituration was discarded after 30 min. The next six to seven triturations were each done for 15 min. Each time, the solution was centrifuged at 500 rpm for 3 min to collect the supernatant and dispersed cells. Resuspension solution was changed every 30 min for solutions containing increasing concentrations of Ca^{2+} (0 to 0.5 mM). The living atrial cell yield was ~30–40%. Only rod-shaped cells with staircase ends, clear cross striations, and surface membranes free from blebs were studied.

Experimental conditions. For the study, an aliquot of cells was transferred onto a polylysine-coated glass coverslip placed at the bottom of a 0.5-ml tissue chamber, which had been mounted on the stage of a Nikon inverted microscope (Nikon Diaphot, Tokyo, Japan). Myocytes were continuously superfused (2–3 ml/min) with normal Tyrode solution containing (in mmol/l) 137 NaCl, 24 $NaHCO_3$, 1.8 NaH_2PO_4, 0.5 $MgCl_2$, 2.0 $CaCl_2$, 4.0 KCl, and 5.5 dextrose (pH 7.4). The solution was bubbled with 5% CO_2-95% O_2. Temperature was monitored continuously and maintained at 19.0 ± 0.5°C for proper voltage control. Patch pipettes were made from borosilicate thin-wall glass (1.5 mm OD and 1.1 mm ID, Sutter Instrument) using a Flaming/Brown-type horizontal puller (model P-87, Sutter Instrument) and polished (type MF-83, Narishige, Scientific Instrument) before use. Pipette resistances ranged between 0.6 and 1.0 MΩ when filled with an internal solution containing (in mmol/l) 125 CsOH, 125 aspartic acid, 20 tetraethylammonium chloride, 10 HEPES, 5 Mg-ATP, 10 EGTA, and 3.6 phosphocreatine (pH 7.3 with CsOH). After the formation of the gigaohm seal, the stray capacitance was electronically nulled. The cell membrane under the pipette tip was then ruptured by a brief increase in suction, forming the whole cell recording configuration. A period of 5–10 min was then allowed for intracellular dialysis to begin before switching to the low Na^+ recording solution containing (in mmol/l) 5 NaCl, 1.2 $MgCl_2$, 1.8 $CaCl_2$, 125 tetraethylammonium chloride, 5 CsCl, 20 HEPES, 11

* S. Baba and W. Dun contributed equally to this study.

Address for reprint requests and other correspondence: P. A. Boyden, Dept. of Pharmacology, Columbia College of Physicians and Surgeons, 630 W. 168th St., New York, NY 10032 (e-mail: pab4@columbia.edu).

The costs of publication of this article were defrayed in part by the payment of page charges. The article must therefore be hereby marked "*advertisement*" in accordance with 18 U.S.C. Section 1734 solely to indicate this fact.

glucose, 3.0 4-aminopyridine, and 2.0 $MnCl_2$ (pH 7.3 with CsOH), designed for proper I_{Na} measurements. With this combination of external and internal solutions, I_{Na} would be of manageable size and isolated from other possible contaminating currents.

Voltage-clamp and recording techniques. Whole cell I_{Na} was recorded using the patch-clamp technique as described (3, 15). Voltage-clamp experiments were performed with an Axopatch 200A clamp amplifier (Axon Instruments). The membrane capacity (in pF) of each cell was measured in the Cs^+-rich solution by integrating the area under a capacitative transient induced by a 10-mV hyperpolarizing clamp step (from −100 to −110 mV) and dividing this area by voltage step. Current amplitude data of each cell were normalized to its cell capacitance (current density, in pA/pF). In cells from adult animals, averaged cell capacitance was 57.6 ± 3.22 pF in RA cells and 104.3 ± 5.2 pF in LA cells. The average time constant of decay of the capacitative transient was 0.11 ± 0.01 ms in RA cells and 0.12 ± 0.01 ms in LA cells. Therefore, the average residual series resistance was 1.95 ± 0.24 and 1.16 ± 0.11 MΩ, respectively. Thus average steady-state voltage error resulting from series resistance was 0.54 ± 0.08 mV for RA and 2.28 ± 0.30 mV for LA ($P < 0.05$). In cells from aged animals, averaged cell capacitance was 79.4 ± 6.0 pF in RA cells and 99.9 ± 8.2 pF in LA cells. The average time constant of decay of the capacitance was 0.14 ± 0.01 ms in RA cells and 0.12 ± 0.01 ms in LA cells. Therefore, the average residual series resistance was 1.87 ± 0.18 and 1.46 ± 0.30 MΩ, respectively. Thus average steady-state voltage error resulting from series resistance was 0.85 ± 0.13 mV for RA and 2.90 ± 0.63 mV for LA ($P = 0.003$).

For consideration of the voltage control, we used 5 mmol/l extracellular Na^+ concentration, maintained at 19 ± 0.5°C, and patch pipettes with resistances no larger than 1.0 MΩ. If experiments demonstrated inadequate voltage control, e.g., a "threshold phenomenon" near the voltage range for Na^+ channel activation and/or an inappropriately steep increase in current amplitude in the negative slope region of the current-voltage relationship curve, data were discarded. Whole cell I_{Na} was obtained by subtracting the traces elicited with comparable voltage steps containing no current (using prepulse to inactivate the Na^+ channels) from the raw current traces

Table 1. *Kinetic properties in adult and aged right and left atrial cells*

	Adult		Aged	
	RA	LA	RA	LA
		Availability		
$V_{0.5}$, mV	−81.6±1.3	−84.4±2.0	−84.5±1.4	−80.8±1.3
k, mV	4.9±0.12	4.9±0.12	4.9±0.08	4.9±0.15
I_{max}, pA/pF	14.8±1.2	23.6±2.3*	18.9±1.7	28.8±4.0*
		Decay at Peak Current		
τ, ms	2.17±0.10	2.01±0.06	2.26±0.09	2.27±0.28
		Time to Peak		
TTP, ms	1.21±0.06	1.26±0.06	1.35±0.06	1.26±0.10
		Recovery at V_h, − 100 mV		
τ_1, ms	31.9±3.5	30.0±2.6	35.2±5.8	26.4±3.5
τ_2, ms	242.1±35.9	168.1±11.6*	254.5±33.2	189.2±35.5
A_1, %	79.3±1.8	79.1±2.3	79.1±1.3	82.3±1.3
		Recovery at V_h, − 90 mV		
τ_1, ms	59.2±6.9	72.6±7.7	59.8±6.4	57.0±8.3
τ_2, ms	317.5±36.7	391.1±41.2	317.0±41.5	340.7±53.0
A_1, %	73.2±2.2	77.3±2.3	70.5±3.5	80.5±1.5*

Values are means ± SE. Adult right atrial free wall cells (RA; $n = 11$), adult left atrial free wall cells (LA; $n = 15$), aged RA ($n = 12$), and aged LA ($n = 10$) were available. $V_{0.5}$ and k, average values of voltage at half-maximal availability and slope factor, respectively, of Boltzmann function best describing data; I_{max}, current density at maximal preconditioning voltage (−140 mV). See Fig. 1 for data collection times. Time course of decay of peak of Na^+ current (I_{Na}) was from currents of current-voltage relations protocol. τ, average time constant of best fit of current decay for cells in each group. In all cells used for peak I_{Na} measurements, time to peak (TTP) of peak current was measured. Time courses of recovery from steady-state inactivation in adult RA ($n = 13$), adult LA ($n = 15$), aged RA ($n = 14$), and aged LA ($n = 13$) were determined by using a conventional double-pulse protocol at holding voltage (V_h) of −100 mV and −90 mV. Current elicited by test pulse was normalized to maximal I_{Na} at interpulse interval of 3,000 ms. τ_1 and τ_2, average time constants of best fits of recovery curves for cells in each group; A_1%, A_1/A_{total}, indicating amplitude of first time constant normalized to total amplitude. *$P < 0.05$, LA vs. RA in both adult and aged groups.

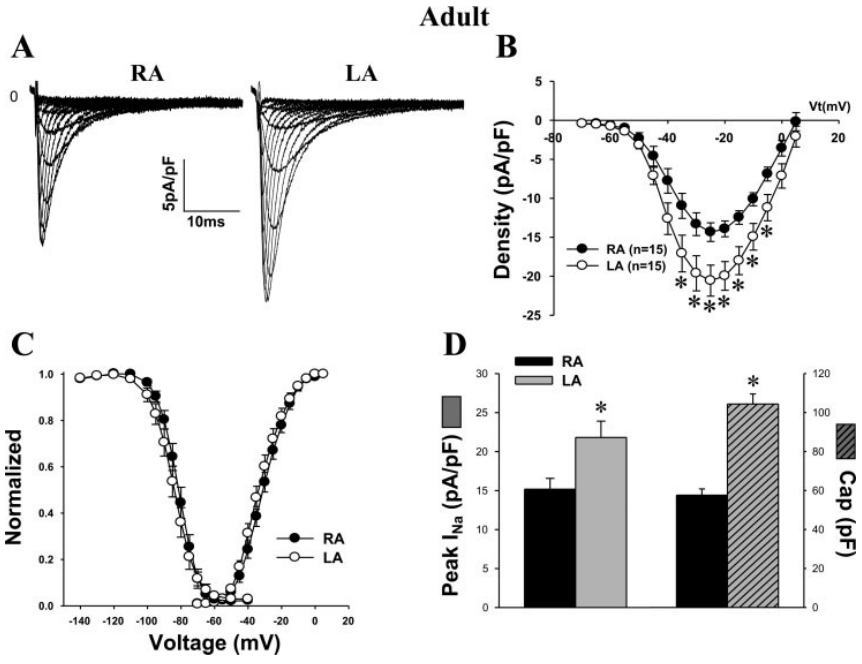

Fig. 1. *A*: family of tracings of Na^+ current (I_{Na}) in adult right (RA) and left (LA) atrial cells. Na^+ currents were elicited from holding voltage (V_h) of −100 mV to various levels of test voltages (V_t) (−70 to +5 mV). *B*: I_{Na} density-voltage relationships in RA and LA. *C*: activation and inactivation curves in RA and LA. Both curves drawn represent best fits of Boltzmann equation for average data points. For activation curves, the half-maximal voltage ($V_{0.5}$) and slope factor k were calculated from current density-voltage (*I-V*) protocol and reversal potential (E_{rev}). In RA, E_{rev} = 5.20 ± 1.11, $V_{0.5}$ = −30.61 ± 1.53 mV, and k = 7.60 ± 0.23; and in LA, E_{rev} = 6.17 ± 0.97, $V_{0.5}$ = −33.10 ± 1.65 mV, and k = 7.38 ± 0.35, $P > 0.05$, RA vs. LA. Data were collected at similar times after whole cell membrane rupture (RA: 18.32 ± 1.72 min, $n = 15$ cells; and LA: 19.03 ± 1.15 min, n = 15 cells, $P > 0.05$). For inactivation curves, a double-pulse protocol was used to determine steady-state inactivation curves. $V_{0.5}$ and k are shown in Table 1. All data were collected at similar times after whole cell rupture (RA: 23.92 ± 0.70 min, $n = 11$ cells; and LA: 25.52 ± 1.08 min, $n = 15$ cells, $P > 0.05$). *D*: summary of peak I_{Na} densities and capacitances (Cap) in RA and LA. Values are means ± SE. *$P < 0.05$, RA vs. LA.

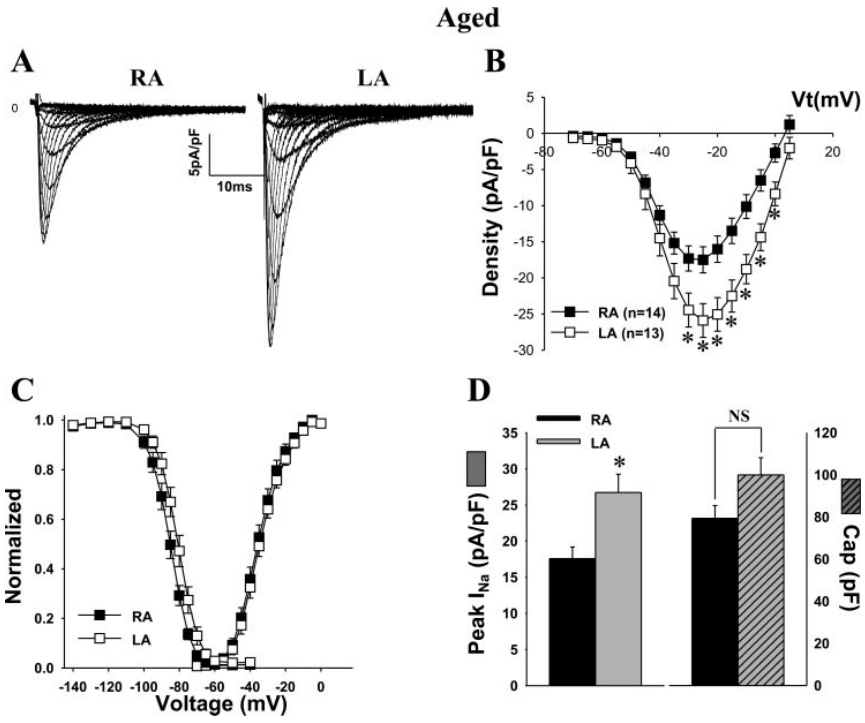

Fig. 2. *A*: family of tracings of I_{Na} in aged RA and LA atrial cells. Na^+ currents were elicited from V_h of −100 mV to various levels of V_t (−70 to +5 mV). *B*: I_{Na} density-voltage relationships in RA and LA. *C*: activation and inactivation curves in RA and LA. Both curves drawn represent best fits of Boltzmann equation for average data points. For activation curves, $V_{0.5}$ and slope factor k were calculated from *I-V* protocol and E_{rev}. In RA, E_{rev} = 3.86 ± 1.07, $V_{0.5}$ = −33.87 ± 1.40 mV, and k = 7.24 ± 0.21; and in LA, E_{rev} = 6.58 ± 0.84, $V_{0.5}$ = −32.37 ± 1.73mV, and k = 7.48 ± 0.35, $P > 0.05$, RA vs. LA. Data were collected at similar times after whole cell membrane rupture (RA: 19.07 ± 1.81 min, n = 14 cells; and LA: 20.54 ± 1.75 min, n = 13 cells, $P > 0.05$). For inactivation curves, a double-pulse protocol was used to determine steady-state inactivation curves. $V_{0.5}$ and k are shown in Table 2. All data were collected at the similar times after whole cell rupture (RA: 23.58 ± 1.50 min, n = 12 cells; and LA: 23.90 ± 0.62 min, n = 10 cells, $P > 0.05$). *D*: summary of peak I_{Na} densities and capacitances in RA and LA. NS, not significant. Values are means ± SE. *$P < 0.05$, RA vs. LA.

(15). In this way, the cell capacitance and linear leakage, if present, were subtracted.

Experimental protocols. Under our conditions, time-dependent changes of Na^+ channel kinetics, including a shift of the availability curve (I/I_{max} curve) in the hyperpolarizing direction have been reported (15). Typically, these changes occur within minutes after membrane rupture. Therefore, peak current data are collected between 15 and 20 min after membrane rupture, and we took care to match the averaged time after membrane rupture at which data were collected for the cells in the two groups (see figure legends). Peak current density in cells from the different groups, *I-V* data, activation data, steady-state availability (I/I_{max}), the time course of inactivation directly from the closed state that is described by two time constants (τ1 and τ2) (see Ref. 15), and time course of recovery of I_{Na} from steady-state inactivation was assessed by using previously published protocols (3, 14, 15).

Table 2. *Kinetic properties in right and left atrial cells*

	Rate of Development of Inactivation of I_{Na} From Depolarized Potential (−60 mV)	
	RA	LA
Adult		
n	17	14
τ_1, ms	41.6±3.5	32.2±4.8
τ_2, ms	143.4±17.8	92.8±14.9
A_1, %	55.7±5.6	58.3±5.3
Aged		
n	13	15
τ_1, ms	27.2±2.9†	42.4±5.1*
τ_2, ms	76.7±6.7†	132.9±17.2*
A_1, %	49.2±6.2	52.5±7.6

Values are means ± SE; n, number of cells. *$P < 0.05$ vs. aged RA. †$P < 0.05$ vs. adult RA.

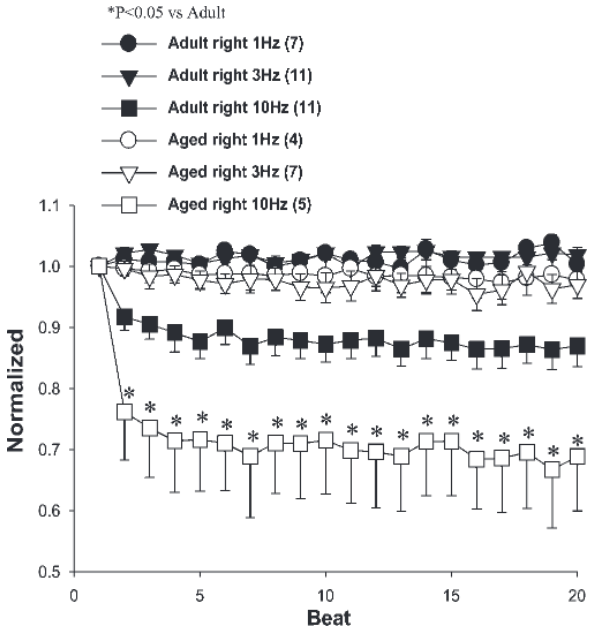

Fig. 3. Use-dependent reduction of I_{Na} in adult and aged RA cells. I_{Na} was elicited by clamp steps from V_h at −100 mV to voltage of peak current for 40 ms at 1-, 3-, 10-Hz pacing rates. Average beat-to-beat reduction of I_{Na} (I/I_{1st}) during 20-pulse train is shown. Use-dependent reduction of I_{Na} was seen in both adult and aged cells at 10 Hz. However, the reduction in aged cells was significantly greater than that in adult cells ($P < 0.05$). n, Number of cells (shown in parentheses).

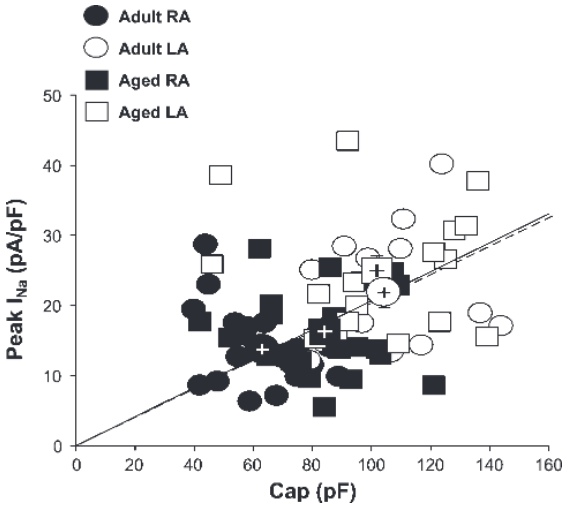

Fig. 4. Relationship of peak I_{Na} densities and capacitances was determined from linear regression to peak I_{Na} densities vs. capacitances. RA (adult, $n = 23$ cells; and aged, $n = 21$ cells) and LA (adult, $n = 15$ cells; and aged, $n = 17$ cells) are shown. Cross-hair big symbols and vertical bars are means ± SE.

In a subset of cells, use-dependent pacing protocols, similar to those described previously (14), were completed to determine whether altered kinetic properties could affect the use dependence of the peak I_{Na}.

Immunocytochemistry. A portion of the cells dispersed for electrical studies were plated on laminin-coated glass chamber slides. Myocytes were fixed with 4% paraformaldehyde for 30 min, rinsed with PBS (Sigma), then blocked in 2% avidin-PBS and rinsed in PBS, and then blocked in 2% biotin-PBS and rinsed in PBS. Myocytes were then incubated with antibodies (diluted 1:15 in PBS containing 0.75% Triton X-100 and 1% normal goat serum) overnight at 4°C. Then myocytes were rinsed in PBS, incubated in biotinylated goat anti-rabbit IgG (diluted 1:300), and rinsed in PBS, incubated in fluorescein avidin D (diluted 1:300), and briefly rinsed in PBS and distilled water. Coverslips were mounted on slides by using aqueous mounting medium (Biomeda, Foster City, CA). Cells were viewed under similar conditions by using Zeiss LSM 410 or Nipkow confocal laser scanning microscope (×60, oil). $Na_v1.5$ immunoreactivity was visualized by 488-nm wavelength of excitation light. Optical sections (1 μm) were taken of each cell.

The antibody recognizing $Na_v1.5$ (13) was a gift from Dr. Catterall's laboratory (Seattle, WA).

Statistics. All values represent means ± SE. A value of $P < 0.05$ was considered statistically significant. For a two-sample comparison, an unpaired *t*-test was used to compare a single mean value between the two independent cell groups. For multiple comparison, an ANOVA was used to determine that the sample mean values between groups were significantly different from each other. If so, a modified *t*-test with Bonferroni correction was used (SigmaStat, Jandel Scientific).

RESULTS

I_{Na} function in RA and LA cells of adult animals. Figure 1 illustrates typical tracings of Na^+ currents under our recording conditions in both an adult RA and LA cell (Fig. 1*A*). Note the similarities in decays of the peak currents (Table 1). Also note that the LA cell I_{Na} density is significantly greater than that of the RA cells at several test voltages (V_t, Fig. 1*B*). In Fig. 1*C*, the average activation and steady-state inactivation curves are plotted. Note that despite the differing density of current, there are no differences in kinetic parameters with the exception of a slight speeding of recovery of LA adult cells (Table 1). Whereas there is a significant difference in peak I_{Na} between RA and LA cells, there is also a significance difference in cell capacitance between cells used in this study (Fig. 1*D*).

I_{Na} function in RA and LA cells of aged animals. Figure 2 illustrates typical tracings of I_{Na} under similar recording conditions in both an aged RA and LA cell (Fig. 2*A*). As for adult cells, LA cell I_{Na} density is significantly greater than that of the RA cells at several V_t (Fig. 2*B*). In Fig. 2*C*, the average activation and steady-state inactivation curves are plotted. Again, note that despite the differing density of current, there are differences neither in decay or time-to-peak parameters nor in the recovery from inactivation (Table 1). However, unlike cells from adult atria, aged LA cells showed kinetic behavior differing from that in aged RA cells when the rate of development of inactivation from a depolarized potential was assessed (Table 2). I_{Na} of aged RA cells tended to enter the inactivated state more readily compared with that of LA cells of aged atria, as well as of their RA counterparts of adult atria. To test whether these kinetic differences would contribute to a rate-dependent effect on I_{Na} and perhaps contribute to conduction characteristics, we tested in a subset of cells the effects of pacing rate on peak I_{Na}. Normalized data are shown in Fig. 3. Averaged individual beat RA data are shown. Note that with pacing at 10 Hz, there is a use-dependent decrease of I_{Na} in adult RA cells (filled squares). This use dependence is significantly greater in aged RA cells (open squares). There was no difference in the use dependence of I_{Na} in LA cells (data not shown).

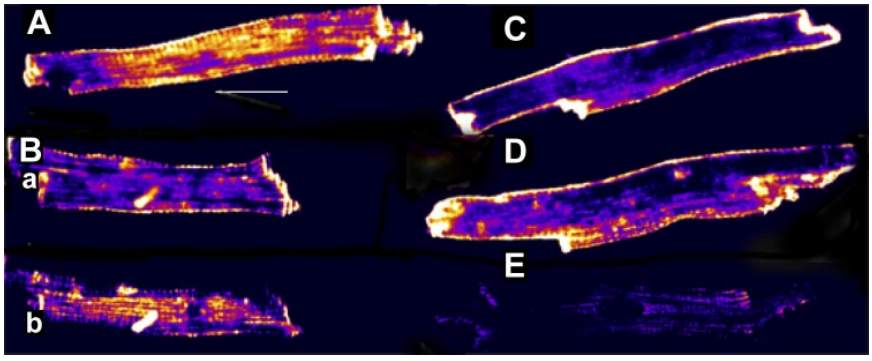

Fig. 5. Immunolocalization of $Na_v1.5$. *A*: $Na_v1.5$ immunolocalization in adult LA (white bar is 25 μm). *B,a* and *B,b*: $Na_v1.5$ immunolocalization in adult RA. Fluorescent staining indicates the presence of $Na_v1.5$ in adult cell surface. *C* and *D*: $Na_v1.5$ immunolocalization in aged LA and RA cells, respectively. Similarly, fluorescent staining indicates the presence of $Na_v1.5$ in aged cell surface. *E*: negative control obtained without primary antibody. All cells imaged at same gain/light intensity.

We next examined whether peak I_{Na} of aged cells differed from those of their adult counterparts. In Fig. 4, peak I_{Na} of each cell was plotted as a function of its capacitance. Average values are depicted by large symbols with cross hairs. There is a correlative relationship ($R = 0.34$, $P < 0.001$) between cell capacitance and I_{Na} density, and average values fall on this relationship; that is, the large cells (predominately LA cells) had large I_{Na}. Average adult cell density values are similar to aged cell values for either atrial chamber [RA: 13.7 ± 1.07 pA/pF in adult ($n = 23$ cells, $N = 13$ preparations), and 16.3 ± 1.3 pA/pF in aged ($n = 21$, $N = 17$), $P = 0.138$; and LA: 21.8 ± 2.1 pA/pF in adult ($n = 15$, $N = 13$), and 26.7 ± 2.5 pA/pF in aged ($n = 17$, $N = 13$), $P = 0.312$].

Immunocytochemistry: $Na_v1.5$ in canine atrial cells. Different from studies using mouse myocytes (13), but similar to a normal ventricular cell study (4), we found that $Na_v1.5$ staining in RA and LA cells from both adult and aged atria was uniform, with staining all along the sarcolemma as well as in the gap junction region (Fig. 5). There was no staining in the cell interior in all cells (Fig. 5 *B,a* and *C*). Thus, although there were electrophysiological differences between RA and LA cells, both cell types showed similar cell-surface staining for the α-subunit of the cardiac Na^+ channel $Na_v1.5$.

DISCUSSION

We report here that there is a significant difference in I_{Na} density between LA and RA cells of adult as well as the aged atria. The reason for this difference is not due to differences in availability or recovery kinetics. It appears that the cell capacitance increase in LA cells is accompanied by increased I_{Na} density. Importantly, in cells isolated from aged animals where P-wave durations are significantly increased (1, 2), Na^+ currents are similar to those we measured in adult atria. I_{Na} density of the aged atria still differed depending upon atrial chamber with LA cell currents being larger than RA cell currents. Thus, with age, the difference in peak I_{Na} between atrial chambers remains. Importantly, we do show an exaggerated use-dependent decrease of peak I_{Na} in aged RA cells. This may contribute to RA conduction abnormalities under some conditions. Finally, we found that there is no structural remodeling of the cardiac Na^+ channel protein $Na_v1.5$ in aged atrial cells.

In a previous study (5), we examined changes in inward and outward currents in aged canine RA cells. In agreement with these studies, we noted that cells from aged animals were large when measured as an increased cell capacitance. However, we reported a decrease in both the average Ca^{2+} and Ba^{2+} current in cells from aged atria (5). Thus the aging process affects I_{Na} and Ca^{2+} current differently. Importantly, we have also shown there to be significant differences in RA outward but not LA outward currents in aged atrial cells (5, 6). Thus aging-associated changes in ionic currents differ, and chamber differences in I_{Na} are maintained in the aged atria.

We have also reported that aging-associated increases in differences in dispersion of APD renders aged atria more susceptible to initiation of arrhythmias and suggested that increased spatial heterogeneity in conduction may provide the basis for unidirectional block. In particular, we noted that the dispersion of V_{max} was significantly greater in aged atria (1), implying marked heterogeneity in conduction in aged atria. However, although these results from Na^+ *I-V* clamp studies may account for the differences in V_{max} between RA and LA cells, our findings cannot account for the increased in conduction abnormalities observed (1, 8, 11) or the slow propagation of premature responses (2), because recovery kinetics of I_{Na} do not appear to change with age. Thus the intrinsic function of the I_{Na} to depolarize the membrane is intact in aged atria and probably does not underlie P-wave changes seen with age. Importantly, although our study is limited in scope, our results are critical and must be considered in the context of results of other studies of aged canine atria. In a recent study (2) using tissues from animals similar to those used here, histological analysis of the atrial freewall showed that muscle bundles were separated by strands of connective tissue (see Fig. 5, Ref. 2), confirming enhanced disposition of connective tissues in aged atria (see also Refs. 8 and 11). Such atrial wall changes may reduce cell coupling and promote discontinuous conduction (16). On the other hand, others have reported a change in the ratio of connexin40 to 43 in the aged atrium (9, 10), suggesting connexin remodeling may be a component of the observed conduction changes observed with age. Unfortunately, none of these previous studies reported on Na^+ channel function in atrial cells from aged atria as we have done here.

Limitations. These data result from cells that are dispersed from very specific regions of the RA and LA. This was done to make a clear comparison to test our hypotheses. Other areas of the atria may differ in their response to age (e.g., pulmonary vein or coronary sinus cells), and such changes may account for differences in triggering between aged and adult atria. We have assessed intrinsic I_{Na} function in cells that could help to provide the substrate for an atrial fibrillation. These studies are not of I_{Na} function in aged animals in the presence of atrial fibrillation.

GRANTS

This study was supported by National Heart, Lung, and Blood Institute Grant HL-67449.

REFERENCES

1. **Anyukhousky EP, Sosunov EA, Chandra P, Rosen TS, Boyden PA, Danilo P Jr, and Rosen MR.** Age-associated changes in electrophysiologic remodeling: a potential contributor to initiation of atrial fibrillation. *Cardiovasc Res* 66: 353–363, 2005.
2. **Anyukhousky EP, Sosunov EA, Plotnikov A, Gainullin RZ, Jhang JS, Marboe CC, and Rosen MR.** Cellular electrophysiologic properties of old canine atria provide a substrate for arrhythmogenesis. *Cardiovasc Res* 54: 462–469, 2002.
3. **Baba S, Dun W, and Boyden PA.** Can PKA activators rescue Na channel function in epicardial border zone cells that survive in the infarcted canine heart? *Cardiovasc Res* 64: 260–267, 2004.
4. **Baba S, Dun W, Cabo C, and Boyden PA.** Remodeling in cells from different regions of the reentrant circuit during ventricular tachycardia. *Circulation* 112: 2386–2396, 2005.
5. **Dun W, Yagi T, Rosen MR, and Boyden PA.** Calcium and potassium current function in right atrial cells from normal and aged canine atria. *Cardiovasc Res* 58: 526–534, 2003.
6. **Dun W, Baba S, and Boyden PA.** Aged-related changes in transient outward and sustained currents in canine right atrial freewall cells are not seen in left atrial cells. *Keystone Symposia: Molecular Pathology of Cardiac Arrhythmias*, 2003.
7. **Feng J, Yue L, Wang Z, and Nattel S.** Ionic mechanisms of regional action potential heterogeneity in the canine right atrium. *Circ Res* 83: 541–551, 1998.
8. **Hayashi H, Wang C, Miyauchi Y, Omichi C, Pak HN, Zhou S, Ohara T, Mandel WJ, Lin SF, Fishbein MC, Chen PS, and Karagueuzian HS.** Aging-related increase to inducible atrial fibrillation in the rat model. *J Cardiovasc Electrophysiol* 13: 801–808, 2002.

9. **Jones SA, Lancaster MK, and Boyett MR.** Ageing-related changes in connexins and conduction within the sinoatrial node. *J Physiol* 560: 429–437, 2004.
10. **Kanagaratnam P, Rothery S, Patel P, Severs NJ, and Peters NS.** Relative expression of immunolocalized connexins 40 and 43 correlates with human atrial conduction. *J Am Coll Cardiol* 39: 116–123, 2002.
11. **Koura T, Hara M, Takeuchi S, Ota K, Okada Y, Miyoshi S, Kodama I, and Ogawa S.** Anisotropic conduction properties in canine atria analyzed by high resolution optical mapping: preferential direction of conduction block changes from longitudinal to transverse with increasing age. *Circulation* 105: 2092–2098, 2002.
12. **Lue WM and Boyden PA.** Abnormal electrical properties of myocytes from chronically infarcted canine heart. Alterations in V_{max} and the transient outward current. *Circulation* 85: 1175–1188, 1992.
13. **Maier SK, Westenbroek RE, Schenkman KA, Feigl EO, Scheuer T, and Catterall WA.** An unexpected effect for brain type sodium channels in coupling of cell surface depolarization to contraction in the heart. *Proc Natl Acad Sci USA* 99: 4073–4078, 2002.
14. **Pu J, Balser J, and Boyden PA.** Lidocaine action on sodium currents of ventricular myocytes from the epicardial border zone of the infarcted heart. *Circ Res* 83: 431–440, 1998.
15. **Pu J and Boyden PA.** Alterations of Na^+ currents in myocytes from epicardial border zone of the infarcted heart. A possible ionic mechanism for reduced excitability and postrepolarization refractoriness. *Circ Res* 81: 110–119, 1997.
16. **Spach MS and Dolber PC.** Relating extracellular potentials and their derivatives to anisotropic propagation at a microscopic level in human cardiac muscle: evidence for electrical uncoupling of side-to-side fiber connections with increasing age. *Circ Res* 58: 356–371, 1986.
17. **Yagi T, Pu J, Chandra P, Hara M, Danilo P Jr, Rosen MR, and Boyden PA.** Density and function of inward currents in right atrial cells from chronically fibrillating canine atria. *Cardiovasc Res* 54: 405–415, 2002.